A MODEL-BASED APPROACH FOR EVENT DEFINITION IN SUPPORT OF FLIGHT DATA MONITORING

Alek Gavrilovski, Dimitri N. Mavris, Georgia Institute of Technology, Atlanta, GA, USA

Abstract

Flight data monitoring (FDM) systems promise safety improvements in flight operations through the use of on-board data from regular flights. FDM systems can provide data pertaining to many types of accidents where human factors have been implicated because they track the manner in which the vehicles are operated. For helicopters, most implementations of such systems on helicopters rely on experts to determine pre-set limits on combinations of flight parameters. These limits are also known as “safety events”. A common practical problem that arises in FDM systems is the need to have sufficient knowledge of a condition before events can be defined and used in a proactive manner. There has been recent interest in using alternative approaches to detecting faults and unsafe events in aviation and solve this inherent limitation of FDM. In this work, a model-based approach is investigated for potential improvements to FDM practices through an objective analysis of the conditions that pertain to an accident. First, a rollover during taxi is investigated using a lateral dynamic model. Various scenarios are passed to the model and analyzed to identify the combinations of conditions that lead to a rollover. The result is a map between the input space and the outcome generated by the model, which can be used by analysts to define boundaries of safe operation. The second model is based on helicopter performance theory and is used with autorotation data. Using estimates of parameters which are not present in the data, an improved detection of existing conditions was achieved. These results suggest that models which contain the appropriate physics may provide potential benefits in generating safety information and enhance the performance of typical helicopter flight data monitoring systems.

ACRONYMS AND NOMENCLATURE

AAIB = Air Accidents Investigation Branch
CAA = Civil Aviation Authority
CI = Condition Indicator
EHEST = European Helicopter Safety Team
FDA = Flight Data Analysis
FDM = Flight Data Monitoring
FDR = Flight Data Recorder
FOQA = Flight Operations Quality Assurance
GPS = Global Positioning System
HFDM = Helicopter Flight Data Monitoring
HUMS = Health and Usage Monitoring System
IHST = International Helicopter Safety Team
NTSB = National Transportation Safety Board
PEGASAS= Partnership to Enhance General Aviation Safety Accessibility and Sustainability
R-ASIAS = Rotorcraft Aviation Safety Information Analysis and Sharing
RPM = Revolutions Per Minute
SMS = Safety Management System

A = rotor disk area
C_{d0} = section zero-lift drag coefficient
C_{PTR} = Tail rotor power coefficient
C_Q = Torque coefficient
C_T = Thrust Coefficient
f = equivalent flat plate drag area
k = force coefficient in the y direction
K = blade profile power correction factor
P = Power
Q = Torque
λ = non-dimensional inflow
λ_c = inflow due to climb
μ = advance ratio
σ = rotor solidity
W = fuselage width
H = fuselage height
m = helicopter mass
d = oleo deflection
d_0 = oleo break-point
I = rotational inertia
$K1_{strut}$ = oleo spring stiffness
$K2_{strut}$ = oleo spring stiffness

K_{tire} = tire stiffness
K_{hub} = hub spring stiffness
$C1_{strut}$ = oleo damping
$C2_{strut}$ = oleo damping
C_{tire} = tire damping
τ_{mr} = main rotor thrust time constant
τ_{tr} = tail rotor thrust time constant
τ_{ϕ} = main rotor tilt time constant

1. INTRODUCTION

Helicopters are extremely useful flying machines, yet seem to suffer from a poor safety reputation, both due to the perception of mechanical unreliability and their regular involvement in high-risk operations[1]. Unfortunately, accident statistics tend to support this claim, especially when compared to commercial airlines[2]. As a result, various organizations have joined in collaborative efforts to facilitate and promote safety efforts across the industry. In addition, helicopter safety has been placed on the NTSB's Most Wanted List[3] of transport system safety improvements, in both 2014 and 2015.

Since its formation in 2005, the IHST[4] and other related groups [5,6] have promoted Helicopter Flight Data Monitoring (HFDM) as one of the primary ways for achieving helicopter safety improvement. By allowing operators to analyse and act upon safety information based on objective flight data, HFDM has the potential to limit exposure to conditions which are otherwise difficult to assess. This benefit has been demonstrated very clearly in some of the early studies on the Helicopter Operations Monitoring Programme [7,8], as well as follow on efforts among additional operators [9]. A recent study by the European Helicopter Safety Team (EHEST) highlighted HFDM as one of its recommended technological means of improving helicopter safety [10]. In addition, the increasing availability and decreasing cost of such recording devices has enabled a much larger number of rotorcraft to be equipped with such recorders, with some manufacturers including them as standard equipment[11].

This work is concerned with the assessment of a potential approach to circumvent certain limitations inherent in HFDM systems, stemming from the fact that most practical implementations rely on the detection of so called safety events. These safety events are represented by thresholds on parameters in the flight data, and generate an indication within the system when exceeded. The rest of the paper is organized as follows: Section 2 provides a brief overview of a typical HFDM system and the practical problems which are considered in this work. Section 3 describes the model-based approach and results pertaining to the limitations identified in Section 2. Finally, our conclusions and future work are summarized in Section 4.

2. BACKGROUND

2.1. Safety improvement potential of HFDM

Over the years, helicopter reliability has been improved significantly, with corresponding increase in safety as evidenced through lower accident rates due to mechanical causes. Though improvements are still being realized, the industry's more recent safety efforts have not been rewarded with sufficiently rapid decreases in accident rates[4]. Several recent surveys of accident statistics support the notion that the primary causes of helicopter accidents are no longer of mechanical nature, but can be traced to decisions made by the crew. While this may be the case, it is also possible that traditional accident analyses aggregate unknown accident causes into the pilot error or loss-of-control category. The following table shows the percentage of all accidents attributable to crew / pilot related actions.

Table 1 Percentage of accidents with crew related causes

Source	Years covered	# accidents	% pilot action
Iseler & Maio [2]	1990-1996	756[1)]	70
Harris, Franklin and Kasper[12]	1963-1998	7618[1)]	64
EHEST[13]	2000-2005	311	70
US JHSAT[14]	2001,2002 & 2006	523	84

The high proportion of accidents in which the crew have been implicated point to the potential for safety improvements through the use of any system that provides insight into the crews' actions, and HFDM in particular.

2.2. The typical HFDM process

HFDM is made possible through the use of on-board data recorders which collect information on flight operational aspects that are otherwise difficult to assess[15]. These recorders are designed to make the information available for analysis much sooner than is possible with legacy FDR equipment. The data are then processed by an analysis system, which checks for the presence of "safety events", conditions which have been deemed noteworthy from a safety perspective and are usually related to

[1)] Number reported for single-engine helicopters

standard operating procedures, regulations, operating envelopes of the vehicle, past accidents and general aviation practices[7,16]. The set of safety events used by an HFDM system is usually stored in a database of events, which must be developed prior to the system becoming operational. Following the analysis, the typical system can generate notifications for immediate action if a high severity event is detected. For more benign events, the presence of events is recorded and monitored over time so that any adverse safety trends can be identified through increases in event detections. In Figure 1, a representative HFDM system layout is shown, based on the system descriptions given in published HFDM guidance documents[15,16].

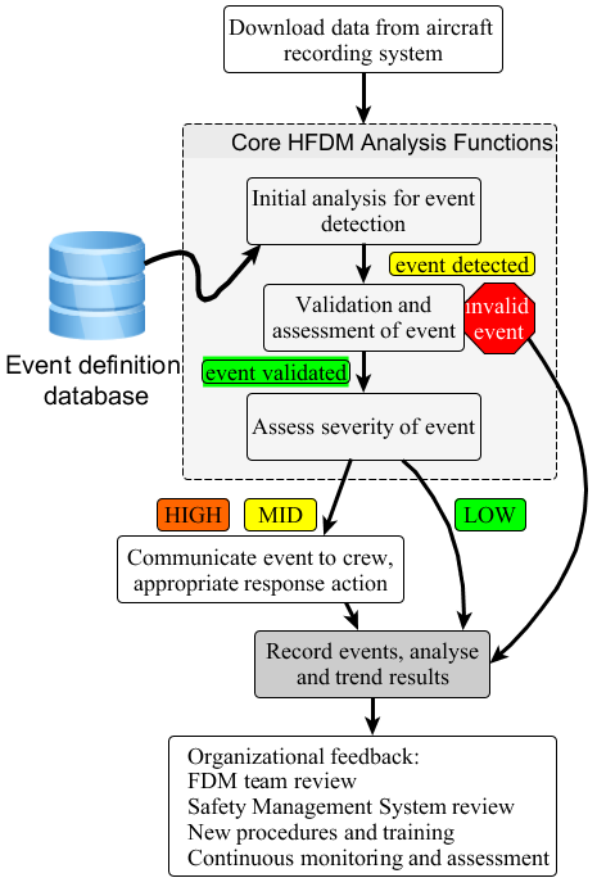

Figure 1 Representative HFDM system layout

The use of thresholds to detect undesirable conditions within the data assumes the existence of an extensive set of such events on which the analysis can be based. A primary challenge for any new HFDM program is the development of this set of events, and their fine tuning to reflect the operator's desired level of safety and operational characteristics. Without a relevant set of safety events, an HFDM system cannot reliably detect undesirable conditions in the data and focus analyst attention to the most safety-critical aspects of the operation. When the number of false alerts is high, the performance of the whole HFDM system diminishes and the real-world safety of the helicopters monitored using this system is affected.

Other inherent limitations with HFDM events can be found in the precursor system to most HFDM, the Health and Usage Monitoring System [17,18]. HUMS utilize a related approach where data recorded from sensors mounted to critical components are used to monitor the performance of the system[17]. A recent article describes how the crew of an EC225 performed a safe ditching manoeuvre after the onboard sensors indicated main gearbox failure[19]. The article also notes that adverse trends had already been recorded by the HUMS data in the flight hours preceding the failure. The basic functionality of HFDM is achieved in a similar fashion to HUMS, through the use of Condition Indicators (Cis) based on features constructed from the data. Most of the components monitored by HUMS have well-defined operational profiles, which allow the calculation of the mean and a narrow variance band which can be taken as the nominal value. Following continued operation and the occurrence of a fault, the monitored signal (usually vibration) exhibits some qualitative shift that can be detected with the HUMS analysis function.

In the case of HUMS, fixed thresholds can provide adequate detection performance because the component condition indicator signal is well defined, with a stable mean and nearly constant variance. However, even in such benign cases, there exists a trade-off between false detections and missed alerts. This trade-off is an intrinsic property of the logical tests conducted as part of the HUMS analysis[20]. Figure 2 illustrates this point using a test between two normally distributed populations, and the resulting missed alert/false alarm rates.

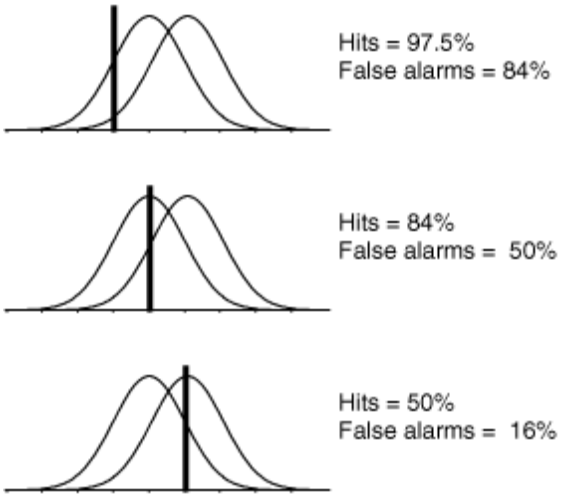

Figure 2 False alerts and missed rates [20]

Dr. Eric Bechhoefer and Dr. Andreas Bernhard[21] discussed some aspects of choosing appropriate threshold values for condition indicators (CIs) based on desired probabilities of false alarms. Their approach uses the fact that the monitored components generate well-behaved signals, and the mean and variance of such signals can reliably be used to define a test statistic with an appropriate balance of false alerts and missed detection[22]. They also showed a way of combining multiple CIs to further reduce the probability of false alerts.

High false alert rates have a negative effect on the performance of an HFDM system by requiring constant fine tuning and detracting analyst resources from more safety critical tasks. On the other hand, a missed detection could potentially result in an incident or accident. An example that has been referred to in HFDM materials is the G-TIGT rollover accident that happened as a result of a confluence of factors, possibly including inappropriate pilot control input. Following a detailed investigation, a safety event was established to detect future approaches to the dangerous condition which contributed to the accident. Both false alerts and missed detections are exacerbated by the type of parameters that are being monitored in HFDM. In particular, most of the data is collected on parameters that have a much more varied spectrum than HUMS measurements, so traditional threshold setting techniques are not directly applicable. Instead, most HFDM events are created by adapting existing events from other operators, creating conditions to monitor against known safety concerns, and other similar heuristics. A list of example events for the helicopters used in the HOMP trials is provided in the final report on that effort[7]. Because the inherent limitations of an HFDM-type system are exacerbated by the characteristics of helicopter operations, an approach is needed that does not rely solely on preconceived safety event definitions to yield information that can be used for safety improvement. In addition, it is desirable to enable detection of safety conditions, with or without safety events.

2.3. Efforts for improvement in HFDM

Much of the research intended to improve performance of HFDM systems has focused on reducing the dependence on pre-defined safety events, with many researchers reporting on some form of a statistical or data mining approach[23,24]. Using the intrinsic structure of the measured data, these data-driven techniques can be used to identify the underlying concepts present and extract meaningful information. Most of the reported efforts are for fixed wing aircraft applications [25,26,27,28,29,30], and show promising results in terms of the ability to detect previously undefined conditions within the data. The fixed wing studies seem to contain an assumption that the majority of operations are of nominal type, and have a narrow variance band so the algorithm can have a good chance of finding anomalies[31]. To accomplish this, the fleet of aircraft used to generate the dataset must also be very uniform.

The researchers also report that the results are usually presented to analysts in order to understand the findings[25,29]. The analysts are thus able to focus on a subset of “interesting” flights/conditions and determine if any unsafe acts or other safety concerns are present.

Another observation is that most of these techniques depend on constructing meaningful features. For example, Li[25] used takeoff and landing profiles, as did Smart[29]. Others developed different features on which to base the analysis. In all of these cases, the construction of features can be equated to encoding prior knowledge of the problem domain.

An alternative approach, model-based monitoring, is a popular way to encode prior knowledge and relate any incoming data to physical characteristics of the system of interest [32]. In this manner, the data analysis is related to realistic properties of the system. Moreover, if the physics are sufficiently well defined, estimates of quantities which aren’t measured in the data can be generated and used to aid the analysis[33]. The technical approach used in this paper is based on this model-based perspective of system monitoring.

3. TECHNICAL APPROACH

The present research seeks to identify some uses of physics-based models in the context of HFDM, and investigate the possibility to use the physics of the helicopter system to aid in defining safe operational bounds for use in HFDM systems. Physics-based models have been very useful in understanding a variety of conditions that relate to helicopter safety. Provided the relevant physics have been described in sufficient detail, such models may reduce the need to collect data at hazardous flight conditions in order to understand the vehicle’s limitations. Some examples include the study of power failure by Carlson and Zhao [34]], who sought to reconstruct a typical H-V diagram using simulation of a tiltrotor. The dynamic rollover study conducted by Fox[35], used a lateral model to investigate the potential for rollover-type accidents and associated damage. Blackwell investigated the interaction of a helicopter touching down on a moving helicopter deck[36]. For a comprehensive discussion of the many uses for models in aerospace system fault diagnostics see Marzat et al[32].

In this work, the focus is on two conditions which have been found to have a high representation

among accidents and incidents, as reported by the NTSB and other research related to the present work[37,38]. The first condition is rollover during ground taxi manoeuvres, similar to the event experienced by G-TIGT[39]. This condition was chosen because it provides an important example of the insight generated after a safety event was implemented in an HFDM system. The second condition considered in this analysis is autorotation. A set of flight data generated during autorotation practice was available to support this analysis. To enable the investigation of these conditions, two separate models were constructed. A simplified dynamic model is used for the analysis of dynamic and static rollover. For the autorotation data, a static performance models with kinematic relationships is used. The following sections describe the structure of the two models and their use, along with relevant results.

3.1. Rollover dynamic model

This initial analysis is focused on developing an understanding of the limits associated with lateral roll dynamics of a helicopter during ground taxi. **A** simplified lateral dynamics model similar to those used by Roy[35] and Blackwell[36] is used for the purpose of studying the lateral behaviour of a helicopter on the ground. The lateral response is critical to estimating the dynamic rollover and other similar conditions. The model contains a rigid body acted upon by forces through the landing gear struts as they come in contact with the ground, and two force vectors representing the main rotor and tail rotor forces. An overview of the model and its components is shown in Figure 3.

3.1.1. Landing gear model

The two main landing gears legs are modelled as oleo struts with non-rigid ground contact points to simulate tire deflections in the ground plane. The following development is presented for one of the main gears, denoted by the subscript a, but the equations are identical for both landing gear legs. The force in the oleo strut is calculated using the following non-linear equation, based on similar expressions used by Blackwell[36]:

$$L = \begin{cases} K_1 d^2 + C_1 \dot{d} & (d < d_0) \\ K_1 d_0^2 + K_2 (d - d_0)^2 + C_2 \dot{d} & (d > d_0) \end{cases} \quad (1)$$

In the above equation, L is the force due to compression of the oleo, d is the oleo deflection, and d_0 is the oleo break-point as defined in[40].

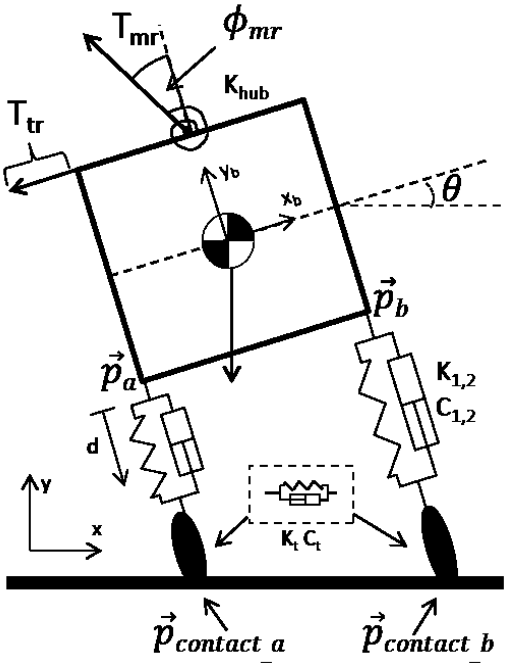

Figure 3 Schematic of rollover model

The strut contact position on the ground, ($\vec{p}_{contact\_a}$ for the left strut), is identified as the point of intersection between the ground and the vector originating at the strut attachment point $\vec{p}_a$ and oriented along the strut in the y direction of the body. The difference between the positions of the strut ground contact point and the strut attachment on the body sets the extension/compression of the oleo strut. The instantaneous closing velocity of the two points is then used to determine the value of the oleo extension/compression velocity.

In addition to the strut contact point, the location of the "tire" contact patch is also determined. The two positions are identical when the vehicle is not in contact with the ground. On the ground, the difference in the two positions account for tire deflection, as described in Blackwell[36]. The following equation determines the side force at the strut ground contact point $\vec{p}_{contact\_a}$ due to tire deflection for contact without sliding:

$$F_{tire\_a} = -K_t (x_{patch\_a} - x_{contact\_a}) - C_t \dot{x}_{contact\_a} \quad (2)$$

In this equation, the location of the contact patch is propagated as a model state when the equations of motions are integrated in time. The contact patch location does not change when the friction force is below the static friction limit, and follows the lateral motion of the strut contact point $\vec{p}_{contact\_a}$ when the static friction limit is exceeded. If the strut separates from the ground, a first-order lag with a small time

constant is used to drive the tire deformation to zero.

$$(3)\quad Fx_a = \begin{cases} F_{tire\_a} & |F_{tire\_a}| < \mu Fy_a \\ sign\left(F_{tire\_a}\right)\mu Fy_a & |F_{tire\_a}| \geq \mu Fy_a \end{cases}$$

In the latter case of Equation (3), the contact patch is moving along with the strut contact point, maintaining maximum friction force. The Fy_a force used in Eq.3 is first calculated for the non-slip condition, and if slip is detected the force is modified.

$$(4)\quad Fy_a = \cos\theta L_a$$

The horizontal and vertical forces at the contact point are then resolved in the body frame, specifically into the frame of the strut, which is aligned with the body in this case. P_a is the force acting at the end of the strut perpendicular to the oleo compression direction:

$$(5)\quad P_a = \cos\theta Fx_a$$

The above equations yield the forces experienced by the end of the landing gear strut over the range of interest. The current analysis assumes a critical angle (60deg.) at which the vehicle has reached an unrecoverable condition, and the calculation of the forces beyond this point is not necessary. Summing the contributions and resolving them in the inertial frame results in the following contribution of the first landing gear strut to the total force acting on the fuselage of the vehicle:

$$(6)\quad F_a = R\begin{bmatrix} P_a \\ L_a \end{bmatrix}$$

In the above equation, R is the rotation matrix that rotates the body to the earth frame by an angle of θ degrees.

The moment due to the landing gear strut can be calculated if the force is multiplied by the instantaneous moment arm about the centre of gravity using the following equation:

$$(7)\quad M_a = \left(\vec{r}_{contact} - \vec{r}_{cg}\right) \times F_a$$

The same calculation is repeated for the other main landing gear strut and the individual contributions are summed in the final calculation of the equations of motion.

3.1.2. Main rotor and tail rotor representation

The next set of forces and moments acting on the vehicle are due to the main rotor and tail rotor systems. For this analysis, both are represented as force vectors with a first-order response to magnitude commands. The main rotor force vector can additionally be tilted by an angle ϕ to represent lateral cyclic commands, which results in a hub moment determined using a torsional hub-spring representation. The force and moment due to the main and tail rotor contributions, resolved in the body frame are:

$$(8)\quad F_{rotors} = R\begin{bmatrix} T_{tr} - \sin(\phi)T_{mr} \\ \cos(\phi)T_{mr} \end{bmatrix}$$

$$(9)\quad M_{rotors} = (\vec{r}_{hub} - \vec{r}_{cg}) \times F_{rotors} + K_{hub}\phi$$

The tail rotor and main rotor forces, along with the direction of the main rotor force vector, are represented as a first-order system within the model. The instantaneous values of these forces are obtained by integrating $\dot{T}_{tr} = (T_{tr\_command} - T_{tr})/\tau_{tr}$ for the tail rotor, and substituting T_{mr}, ϕ_{mr} and associated time constants to obtain the main rotor values. The tail rotor has a shorter time constant to simulate the much faster response to pitch changes, as opposed to main rotor flapping. Also, varying the magnitude of the main rotor orientation time constant can be used to simulate the delay in pilot cyclic input to rolling moment changes due to the tail rotor force. This model is assumed to operate from the trim point with respect to rotor torques, so the results that follow assume the tail rotor force required to balance the main rotor torque has already been applied and is balanced by some lateral main rotor tilt. All further analyses begin from this trim point.

3.1.3. Equations of motion

In addition to the forces due to the landing gear and rotor forces, the helicopter is acted upon by the force of gravity, which is applied in the downward direction at the CG and therefore provides no additional moments. Combining the above expressions gives the final form of the equations of motion for the simplified helicopter rollover model. The equations are resolved in the inertial frame and expressed in terms of the x and y components as shown below:

$$(10)\quad \begin{bmatrix} \ddot{x} \\ \ddot{y} \end{bmatrix} = \frac{1}{m}\left(\begin{bmatrix} 0 \\ -g \end{bmatrix} + R\begin{bmatrix} P_a \\ L_a \end{bmatrix} + R\begin{bmatrix} P_b \\ L_b \end{bmatrix} + R\begin{bmatrix} T_{tr} - \sin(\phi)T_{mr} \\ \cos(\phi)T_{mr} \end{bmatrix}\right)$$

$$(11)\quad \ddot{\theta} = \frac{1}{I}\left(M_a + M_b + M_{rotors}\right)$$

These equations are numerically integrated using a variable time-step integrator to yield the time-domain response of the helicopter. The parameters used in

this initial analysis are shown in Table 2, and can be modified to represent specific vehicles as needed.

Model parameter	Value
W	3 m
H	4 m
m	3000 Kg
d_o	1 m
I	6.25 10^3 Kg m^2
$K1_{strut}$	1.0 10^5 N/m
$K2_{strut}$	1.4 10^5 N/m
$C1_{strut}$	1.5 10^4 N s/m
$C2_{strut}$	1.8 10^4 N s/m
K_{tire}	2.2 10^5 N/m
C_{tire}	3.0 10^4 N s/m
τ_{MR}	0.7 s
τ_{TR}	0.3 s
τ_{ϕ}	1.3 s
K_{hub}	1.95 10^4 N m/rad

3.2. Dynamic model response

The output of the simulation model captures the displacement and orientation of the helicopter and produces results comparable to the model described by Blackwell, with the distinction that the present analysis is concerned with the lateral behaviour. To test the response of the model, the vehicle is "dropped" from a moderate height at several lateral velocities. The vehicle settles in the case where it is dropped vertically and rolls over if sufficient lateral velocity is present at the time of contact. The time histories for three drop scenarios are shown in Figure 4. The modelled response shows a reasonable behaviour that reflects the type of motion expected during a helicopter rollover.

The vehicle reactions to control inputs can be similarly investigated. Once on the ground, the vehicle is allowed to settle for a period of 2 seconds, followed by the application of control inputs. The vehicle reacts by tilting in the direction of the resulting forces and moments. If sufficiently large forces are applied, the vehicle can slide or lift off the ground. Large moment application can result in a rollover of the vehicle, which is detected when the roll angle reaches a set angle, as shown in Figure 5.

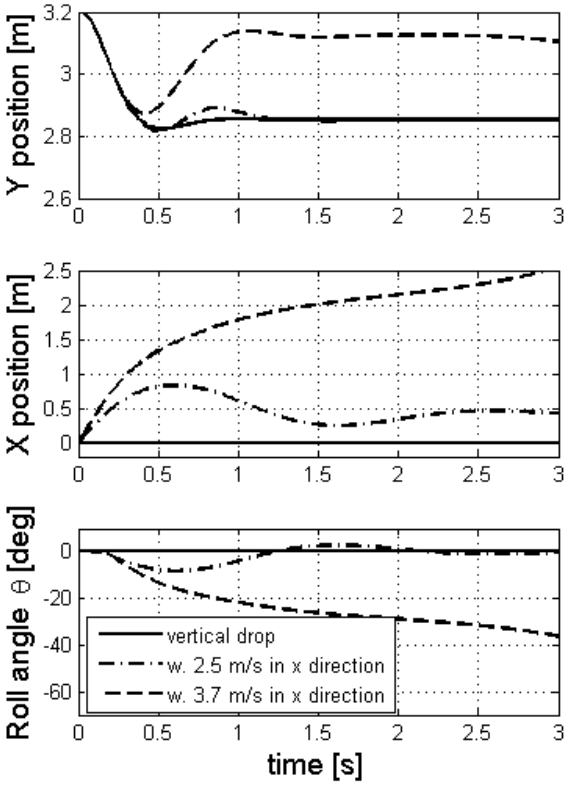

Figure 4 Model responses following drop

The model does not detected collisions explicitly, aside from contact between the landing gear and the ground, but assumes an ultimate roll angle of 60 degrees as the stopping point for the simulation. In reality, parts of the helicopter may come in contact with the ground at lower angles. However, even lower angles may be unrecoverable, a fact which is reflected in the behaviour of the model.

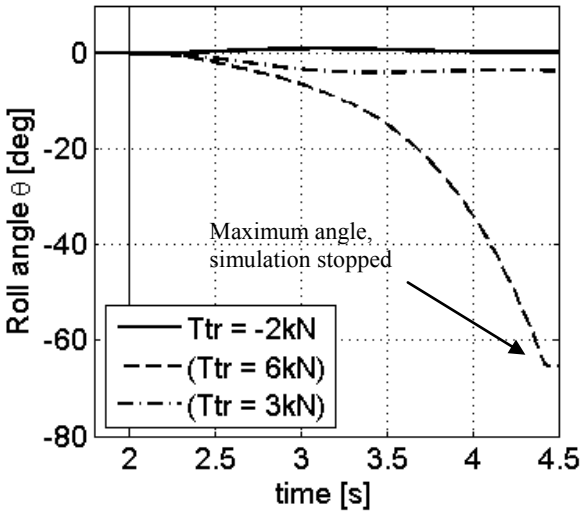

Figure 5 Response to three different TR inputs

The primary purpose for the construction of this model was to investigate the combinations of inputs that result in dynamic and static rollover. To accomplish this, the results of individual simulation runs are analysed to determine if a rollover had occurred. Throughout the analysis, the time required for the helicopter to reach the critical state is tracked, resulting in a measure of safety in terms of time. This can be interpreted as remaining reaction time and is based on similar analyses performed in the automobile industry[41,42]. On the other hand, static rollover occurs at low levels of main rotor thrust and high tail rotor thrust settings, as is the case when a wheeled helicopter is initiating or stopping a taxiing turn. In helicopters with high-mounted tail rotors the moments can be quite significant and aircrews are trained to coordinate their turns using the lateral cyclic control.

3.3. Dynamic rollover

Dynamic rollover occurs when the landing gear constrains the motions of the helicopter by coming in contact with the ground while the main rotor is producing a significant amount of thrust. Since the moment arm is now about the constraining landing gear, and not about the CG, cyclic control inputs are less effective at reducing the roll angle and reversing the rotation. The proper course of action, and the recommended practice, is to immediately reduce collective when dynamic rollover is detected.

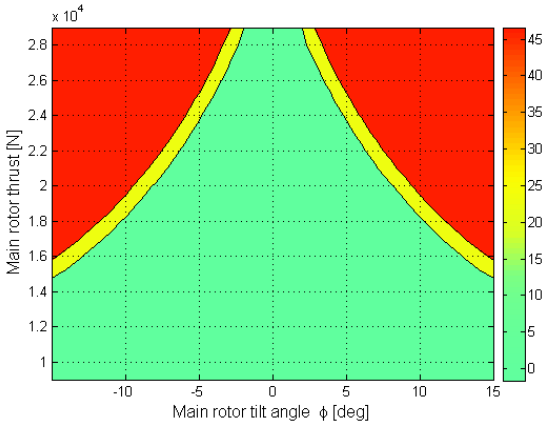

Figure 6 Mapping of main rotor inputs to the dynamic rollover condition

3.4. Static rollover

Static rollover is different from the dynamic case in that it can be achieved using contributions from the tail rotor only, if the tail rotor is sufficiently powerful and is mounted far from the roll axis. Figure 7 shows the angle achieved the simulation as tail rotor command increases. The point where the tail rotor overpowers the stability of the vehicle is indicated in the figure. It is important to note that the angle at which the rollover occurs is lower than the static angle when no forces are applied and the only moment present is due to the weight of the vehicle.

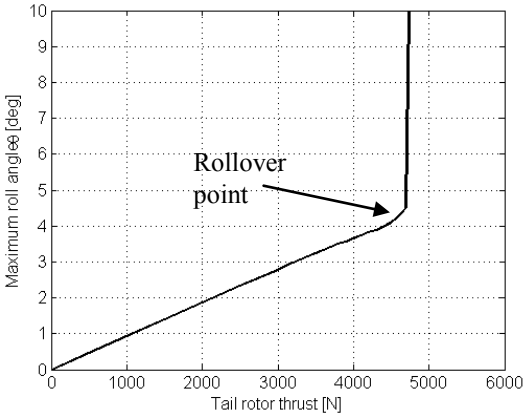

Figure 7 Tail rotor input and maximum angle achieved indicating rollover point

3.5. Combined lateral cyclic and tail rotor pedal application

The simultaneous application of tail rotor pedal and main rotor lateral cyclic and collective inputs causes the vehicle to tilt in the direction of the applied forces and moments. In helicopters with a high-mounted tail rotor, large and unexpected moments can develop quickly and potentially surprise the crew. Such large moments could lead to a rollover of the helicopter if not corrected, such as the condition described in the official AAIB report on the G-TIGT accident [39,43]. In addition to accidents, evidence seems to support the claim that many more near-misses also occur [43]. The fairly well defined boundary between the safe and rollover regions is shown in Figure 8, where the coloration represents the maximum angle achieved. This mapping of the control inputs to the safety of the outcome could prove useful in setting thresholds for safety events designed to detect similar conditions in the data.

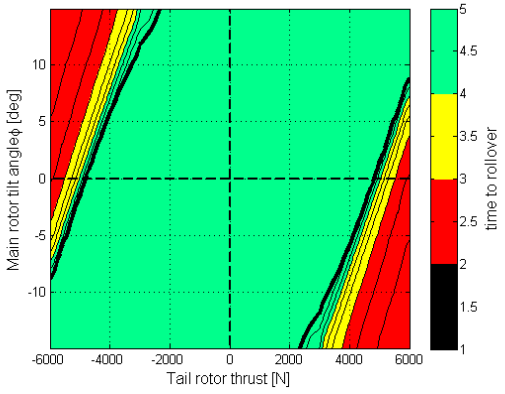

Figure 8 Mapping of combined MR and TR inputs to maximum roll angle achieved

Next, we investigate the effect of the main rotor thrust on the limits of the combined input envelope. Higher thrust settings shrink the set of allowable control inputs where a rollover is not encountered. The modified mapping, defined for three different thrust settings is shown in Figure 9. While the static envelope defined in Figure 8 may be relatively easy to implement in standard HFDM event sets, the thrust-dependent nature limits shown in Figure 9 present a practical challenge. Specifically, most HFDM systems use definitions of the form described with Equation 11 in the following section, which means that dynamic limits are not easily encoded.

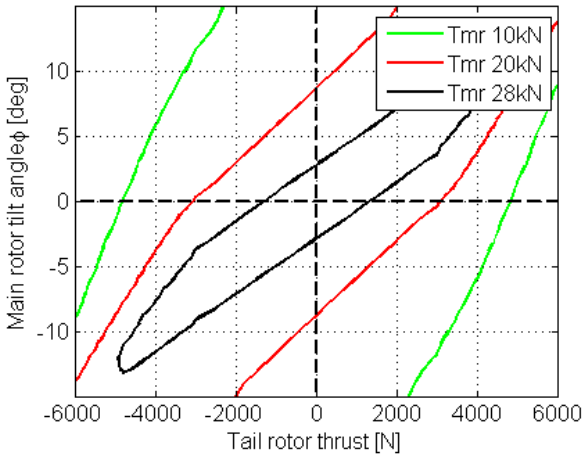

Figure 9 Effect of main rotor thrust on safe input envelope

The envelopes described so far are based on tracking the maximum angle achieved by the simulated helicopter and identifying regions of the input space that result in a rollover. It is possible that for some inputs, the critical angle is possible to reach but the rollover conditon takes longer to develop. Considering the fact the crew is not likely to maintain a constant control input over extended periods, the time required to reach rollover may provide additional insight. Figure 10 shows a comparison between the envelope defined purely based on angle (shown in black line), and the time-to-rollover envelope defined by measuring the period between control application and resulting rollover. This result suggests that incorporating time-based information into the formulation of safe bounds can differ from the purely angle-based definition and yield additional information for conditions which otherwise have the identical outcome in the long term.

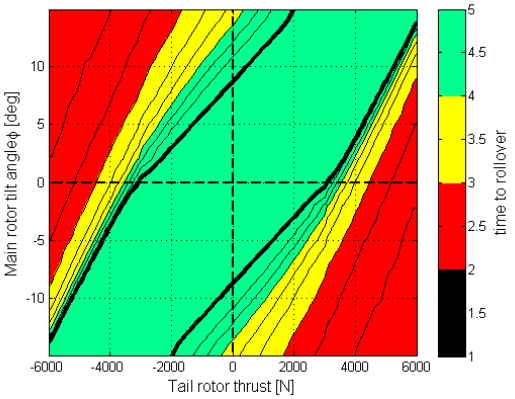

Figure 10 Limits based on time-to-rollover with angle-based limit in black

The limits shown in Figure 10 are representative of the rollover during taxi experienced in the G-TIGT accident. This type of rollover occurs when the crew applies pedal control rapidly, without sufficient coordination using the lateral cyclic. Following the real accident, a detailed study was performed to determine its causes[39] and establish safe operational limits for taxiing. The result of that study were the limits on combined main rotor and tail rotor inputs that were implemented in the HFDM system used by the operator[43]. The period following the implementation of the new event threshold for “near rollover” conditions revealed the relatively high frequency with which such conditions occur.

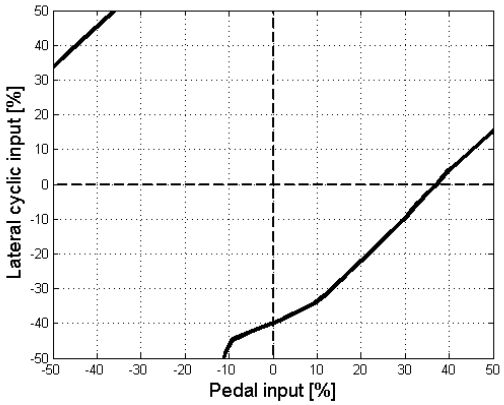

Figure 11 Control input limits defined following accident

Results presented in this section qualitatively resemble the actual limits implemented by the operator following the G-TIGT accident (Figure 11). A direct quantitative comparison is not straightforward, as the limits have been shown without supporting information regarding the weight of the helicopter or thrust setting. It seems reasonable that if the present model is further refined to create a more accurate representation of the

vehicle in question, safe limit boundaries could be defined entirely based on the physics involved. This outcome may lead to future safety event definitions being defined without requiring real-world accident data to precede their development. As such, the dynamic model-based safety event threshold identification may have significant potential to reduce the time required to develop and fine tune events, with corresponding increases in HFDM system effectiveness.

3.6. Autorotation practice performance model

During the course of this study, flight data recorded by a helicopter operator became available and prompted the investigation of an additional condition, which required the implementation of a helicopter performance model. Most of the flight data were collected during uneventful routine flights, but a single flight was identified where large vertical speed deviations had been detected. It was determined that this flight represented practice autorotations. This was confirmed by the fact that the flight data contained associated safety event definitions used by the operator to assess the aircrews' performance during training. Specifically, the limits set by the operator were of the following type, defined for three different levels of severity:

$$\begin{aligned} & Vc < -980\,ft/\min \\ & \quad and \\ & V < 42kts \quad low \\ & V < 36kts\,medium \\ & V < 33kts \quad high \end{aligned} \tag{11}$$

In the above expression, Vc is the climb velocity and V is the horizontal velocity. The above values are close but not exactly the operator's definition, yet the formulation in terms of logical tests at three different forward speeds and a particular descent velocity is identical. The purpose of this event definition is to detect conditions where the descent velocity and horizontal speed combination results in a lower energy state, and could potentially lead to a loss of rotor RPM prior to the landing flare. Maintaining sufficient RPM is critical to safe autorotation, and requires delicate technique, which is why this operator had chosen to monitor practice flights using HFDM. Since the underlying physical phenomenon is related to power extraction by the rotor, a momentum-theory based estimate of the power required in descent was constructed as described in Leishman[44]:

$$\begin{aligned} C_P \equiv C_Q = & \frac{kC_T^2}{2\sqrt{\lambda^2+\mu^2}} + \frac{\partial C_{d0}}{8}(1+K\mu^2) \\ & + \frac{1}{2}\left(\frac{f}{A}\right)\mu^3 + \lambda_C C_T + C_{PTR} \end{aligned} \tag{12}$$

A simple estimate for the ideal autorotative descent speed throughout the range of forward speeds can be obtained if the above equation is expressed in terms of λ_c, the normalized climb velocity. The result is an expression that relates descent velocity to the instantaneous power requirement, so that the descent velocity required to drive the power requirement to zero (or to some negative value) can be calculated. This model makes simplifying assumptions regarding the flight state and vehicle characteristics, such as a constant RPM throughout the autorotation and uniform inflow. There are obvious limitations associated with such assumptions, which will be addressed with future model development and enhanced uses of the flight data. Still, the model provides a good first estimate of a safe boundary which can be used to evaluate existing HFDM safety event definitions.

3.7. Results for autorotation practice

The flight data gathered during the practice autorotation flight comprised a set of in-flight measurements, containing GPS location, ground speed data and acceleration signals. No control input data were available. The flight data for this flight are shown in Figure 12. The upper portion of the graph contains the usual flight phases, such as climb, descent and cruise, which are discernible as denser clustering of points. Below 980 ft/min descent, the vehicle is assumed to have entered autorotation, and the appropriate detection of safety events based on severity is carried out. In the figure, points marked in blue are safe flight conditions, whereas the red points are the most severe excursions from the prescribed descent profile. On the same graph, an estimate of the actual autorotation boundary is also plotted using a thin dashed line. Points that are below this curve are considered safe, since the power required is negative, meaning the rotor is extracting excess energy from the surrounding flow and can sustain its RPM.

An observation based on this comparison is that the original safety event implementation is primarily dependent on changes in velocity, provided that the vertical descent speed threshold is met. Comparison with the descent speed estimate reveals the fact that the implemented limits and the ideal boundary are functionally different. With the assumption that the calculated ideal boundary is in fact the true limit, it becomes clear that the implemented limits result in both missed detection and a large number of false

alerts. The region of blue points is considered safe, yet falls below the minimum descent speed at any forward velocity. Similarly, much of the data classified as low, medium and high severity safety events can be found inside the safe region as defined by the minimum descent speed curve. In fact, the operator data showed that a large number of nuisance alerts were generated, and later dismissed by the analyst. A potential approach to improving the original detection thresholds would be to implement the ideal descent speed limit as the new threshold value. Since this descent speed is calculated for a steady-state cruise condition, a much more relevant analysis would be to calculate the power required for each flight data point.

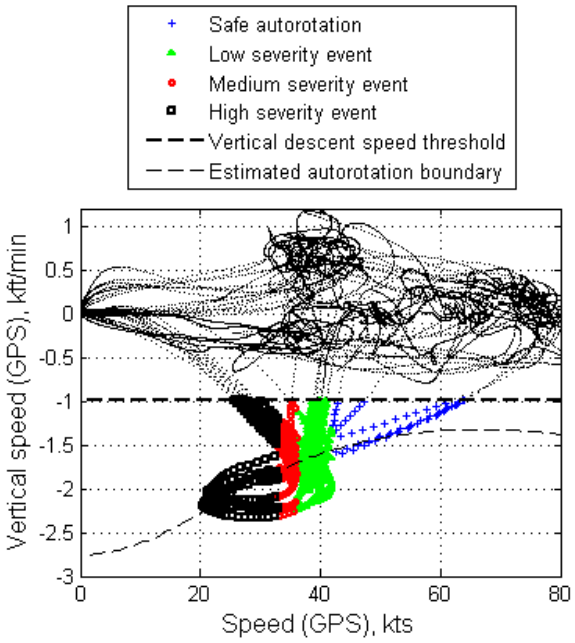

Figure 12 Autorotation training with detected events

This approach was attempted and shown in Figure 13. The model generated an estimated power requirement for each data point. In addition to the horizontal and vertical velocities, information in the form of the helicopter's orientation and acceleration were utilized to derive the instantaneous thrust requirement. The result is an improved estimate of the autorotative state. The transition between safe and unsafe regions occurs primarily in the direction perpendicular to the ideal limit, as shown in the figure.

The coloration and severity of the points is based on the power estimate at each datum. Red points denote conditions where the rotor requires power from the engine, which is assumed unavailable. The yellow points are defined as those that do not require engine power, but extract less than 5% excess power. The green points represent flight conditions with ample excess power available from the airflow.
Another refinement that is possible with the introduction of basic kinematics into the performance model is the estimation of the general wind component

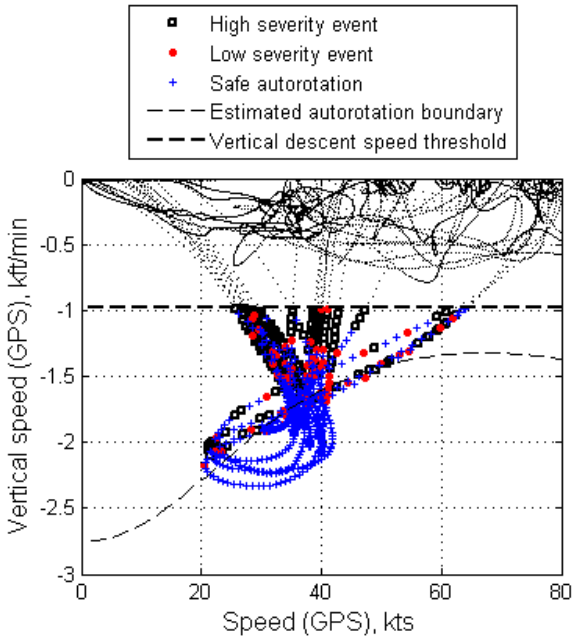

Figure 13 Performance-model used with data

Note that in both Figure 12 and Figure 13, the autorotative portion of the flight is occurring at rather slow forward speeds. It was stipulated that this may be due to a significant wind component present at the time of the flight. In the case of this example flight, a sufficient number of direction changes occurred to allow simple wind estimation. This was accomplished by considering the variability in the ground speed of the cruise segments between autorotations. A clear variation with heading was observed, and the difference between the peak value and the mean cruise speed was taken as the wind velocity. It was estimated that the wind velocity was approximately constant at 18 Kts. The modified model-based safety estimate is shown in Figure 14.
The addition of the wind estimate means the downwind portions of flight have been effectively slowed down, while the upwind sections have a corresponding increase in estimated forward velocity. Most of the points from the flight data which were previously classified as borderline/unsafe, have now been shifted toward the safe part of the descent/forward speed region. Compared to the original detection using the raw flight data, this development means that the nuisance false alarms would be greatly reduced. This final refinement

highlights the fact that a much broader spectrum of information may already be available in existing flight data, yet the threshold-based safety events currently in use rarely make use of this information.

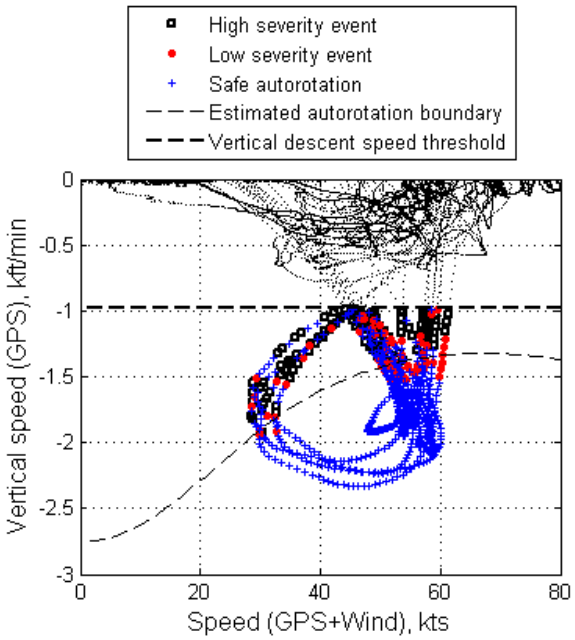

Figure 14 Performance model used on flight data with wind estimate

4. CONCLUSION AND FUTURE WORK

This paper discussed the benefits of HFDM systems and potential approaches to mitigating some inherent limitations. In particular, a model-based approach is proposed to aid in the development of appropriate safety events that can then be used to detect unsafe conditions. It was shown through review of existing material and simple performance examples that mismatches between functional forms of detection thresholds and the underlying condition can contribute to the problem of false alarms and missed detections.

Based on this brief exploration, we showed two potential uses for physics based helicopter models. In the case of the rollover during taxi, a simplified model was shown to reconstruct boundaries that qualitatively resemble the limits defined in a real HFDM system following an accident. In the second case, a simple performance model was used to provide an estimate of power requirements during autorotation, which has the potential to improve detection of autorotation and also take into account a range of previously unused information. These results can be interpreted by analysts to help define safety events for use in HFDM detection, with improved accuracy and reduced effort and rework.

This work was an initial investigation into the potential uses of dynamic and performance models in the context of HFDM. The primary goal was to address limitations in HFDM and extract greater information from the flight data by incorporating knowledge of the system's physical properties. Another benefit is the potential for generating event limit thresholds without requiring data to support that development. At present, the results of these analyses are left for interpretation by an analyst. In the longer term, a more optimal technique would be considered. An obvious limitation of the present approach is that the physics that belie the real system must be captured appropriately. For the limited cases discussed in this work, the present models are seen as adequate, but further work will be required to extend the analysis to additional conditions. For example, if the dynamic model and performance model are to be unified, a full helicopter simulator will be the logical next step. Any additional effects would have to be explicitly modelled. However, the initial results seem to support the use of physics-based models and the ability to explore the range of operational conditions may as a viable path to pre-emptively defining event thresholds for use in HFDM.

ACKNOWLEDGEMENTS

This work was sponsored by the Federal Aviation Administration under Project No. 2 "Rotorcraft Aviation Safety Information Analysis and Sharing" of the FAA Center of Excellence for General Aviation, PEGASAS (Partnership to Enhance General Aviation Safety Accessibility and Sustainability), via grant No. 12-C-GA-GIT-003 to the Georgia Institute of Technology. The authors are grateful to FAA project technical monitor Mr. Charles Johnson. The information in this research does not constitute FAA Flight Standards or FAA Aircraft Certification policy.

5. REFERENCES

[1] Burgess, Scott, “The Reality of Aeronautical Knowledge:The Analysis of Accident Reports Against What Aircrews are Supposed to Know”, 2012, url: http://www.ihst.org/portals /54/Reality_Aeronautical_Knowledge_21MAY12.pdf, accessed 7/12/2015

[2] Iseler, Laura, And Joe De Maio. "Analysis Of US Civil Rotorcraft Accidents From 1990 To 1996 And Implications For A Safety Program." Annual Forum Proceedings-American Helicopter Society. Vol. 57. No. 2. American Helicopter Society, Inc, 2001.

[3] National Transportation Safety Board, “NTSB Most Wanted List 2014: Address Unique Characteristics of Helicopter Operations,” url http://www.ntsb.gov/safety/mwl/Pages/default.aspx accessed 7/15/2015

[5] EHEST,”EHEST” url: http://easa.europa.eu/essi/ehest/, accessed 7/1/2015

[6] Global HFDM Steering group,”Home”, url: HFDM.org accesed 7/15/15

[7] Larder, B. D. "Final Report on the Helicopter Operations Monitoring Programme (HOMP) Trial." CAA Paper 2 (2002): 25.

[8] Civil Aviation Authority, “Final Report on the Follow-on Activities to the HOMP Trial,” 2004.

[9] J. Doerflinger, G. Bruniaux, P. Pezzatini, M. Greiller, and J. Marcellet, “Small Helicopter Operational Monitoring Programme (HOMP) Trial,” 2010.

[10] J. M. G. F. Stevens and J. Vreeken, “The Potential of Technologies to Mitigate Helicopter Accident Factors – An EHEST Study,” 2014.

[11] Rotor On Line, “Helicopter Flight Data Monitoring and the Alerts Vision 1000 System”. url: http://www.airbushelicopters.com/w1/jrotor/82/pageLibre0001009a.html accessed 7/10/2015

[12] Harris, Franklin D., Eugene F. Kasper, and Laura E. Iseler. “US civil rotorcraft accidents, 1963 through 1997”. No. NASA-A-0004325. NATIONAL AERONAUTICS AND SPACE ADMINISTRATION MOFFETT FIELD CA AMES RESEARCH CENTER, 2000.

[13] European Helicopter Safety Team, “Analysis of 2000-2005 European Helicopter Accidents,” Cologne, Germany, 2010.

[14] U.S. Joint Helicopter Safety Analysis Team, “The Compendium Report: The U. S. JHSAT Baseline of Helicopter Accident Analysis Volume I,” 2011.

[15] U.S. JHSIT, “HELICOPTER FLIGHT DATA MONITORING TOOLKIT,” pp. 1–22, 2011.

[16] CAA, “CAP 739 Flight Data Monitoring”,url: http://www.caa.co.uk/docs/33/CAP739.pdf, accessed 7/9/2015

[17] U.S. JHSIT, “Health and Usage Monitoring Systems Toolkit,” 2013, url: http://www.ihst.org/portals/54/Toolkit_HUMS.pdf, acessed 7/15/2015

[18] Dempsey, Paula J., et al. Rotorcraft health management issues and challenges. National Aeronautics and Space Administration, Glenn Research Center, 2006.

[19] AIN article about http://www.ainonline.com/aviation-news/aviation-international-news/2012-06-02/ec225-ditches-safely-north-sea-probe-centers-gearbox

[20] Da*vid* Heeger. “Signal Detection Theory Handout”,url: http://www-psych.stanford.edu/~lera/psych115s/notes/signal/. Accessed 7/12/2015

[21] E. Bechhoefer and A. P. F. Bernhard, “Setting HUMS Condition Indicator thresholds by modeling aircraft and torque band variance,” IEEE Aerosp. Conf. Proc., vol. 6, pp. 3590–3595, 2004.

[22] Byington, Carl S., et al. "Metrics evaluation and tool development for health and usage monitoring system technology." Third International Conference on Health and Usage Monitoring-HUMS2003. 2003.

[23] Friedman, Jerome, Trevor Hastie, and Robert Tibshirani. The elements of statistical learning. Vol. 1. Springer, Berlin: Springer series in statistics, 2001.

[24] Chandola, Varun, Arindam Banerjee, and Vipin Kumar. "Anomaly detection: A survey." ACM computing surveys (CSUR) 41.3 (2009): 15.

[25] Li, Lishuai, et al. "Anomaly Detection In Onboard-Recorded Flight Data Using Cluster Analysis." Digital Avionics Systems Conference (Dasc), 2011 IEEE/AIAA 30th. IEEE 2011.

[26] Iverson, David L. "Inductive System Health Monitoring With Statistical Metrics." Proceedings Of The 4th JANNAF Modeling & Simulation Subcommittee (MSS) Meeting. 2005.

[27] MUGTUSSIDIS, IOSSIF B., MARK R. ANDERSON, AND FAQS BY INSTITUTIONS. "A CLUSTERING METHOD FOR FLIGHT DATA REDUCTION." PROCEEDINGS OF AIAA GUIDANCE AND NAVIGATION CONFERENCE, AIAA. VOL. 4483. 2000.

[28] Budalakoti, Suratna, Ashok N. Srivastava, And Matthew Eric Otey. "Anomaly Detection And Diagnosis Algorithms For Discrete Symbol Sequences With Applications To Airline Safety." Systems, Man, And Cybernetics, Part C: Applications And Reviews, IEEE Transactions On 39.1 (2009): 101-113.

[29] Smart, Edward, and Dean Brown. "A Two-Phase Method Of Detecting Abnormalities In Aircraft Flight Data And Ranking Their Impact On Individual Flights." Intelligent Transportation Systems, IEEE Transactions On 13.3 (2012): 1253-1265.

[30] Das, Santanu, et al. "Multiple Kernel Learning For Heterogeneous Anomaly Detection: Algorithm And Aviation Safety Case Study." Proceedings Of The 16th ACM SIGKDD International Conference On Knowledge Discovery And Data Mining. ACM, 2010.

[31] Gorinevsky, Dimitry, Bryan Matthews, and Rodney Martin. "Aircraft anomaly detection using performance models trained on fleet data." *Intelligent Data Understanding (CIDU), 2012 Conference on*. IEEE, 2012.

[32] Witczak, Marcin. *Modelling And Estimation Strategies For Fault Diagnosis Of Non-Linear Systems: From Analytical To Soft Computing Approaches*. Vol. 354. Springer Science & Business Media, 2007.

[33] Marzat, Julien, et al. "Model-based fault diagnosis for aerospace systems: a survey." Proceedings of the Institution of Mechanical Engineers, Part G: Journal of Aerospace Engineering (2012): 0954410011421717.

[34] Carlson, Eric B., and Yiyuan J. Zhao. "Prediction of tiltrotor height-velocity diagrams using optimal control theory." Journal of aircraft 40.5 (2003): 896-905.

[35] Fox, Roy G. Lateral Rollover Protection Concepts. BELL HELICOPTER TEXTRON FORT WORTH TX, 1980.

[36] Blackwell, Jeremy, and R. A. Feik. A mathematical model of the on-deck helicopter/ship dynamic interface. No. ARL-AERO-TM-405. AERONAUTICAL RESEARCH LABS MELBOURNE (AUSTRALIA), 1988.

[37] NTSB, “NTSB Aviation Accident Database”, online query; url: http://www.ntsb.gov/_layouts/ ntsb.aviation/index.aspx, accessed 7/10/2015

[38] Arjun H. Rao and Karen Marais,”Identifying High-Risk Occurrence Chains in Helicopter Operations from Accident Data”; 15th AIAA Aviation Technology, Integration, and Operations Conference. June 2015

[39] Aviation Accident Investigation Branch, “Aerospatiale AS332L Super Puma , G-TIGT , 4 January 1996,” 1996. url: https://assets.digital.cabinet-office.gov.uk/ media/5422f25340f0b6134600042d/ dft_avsafety_pdf_501327.pdf; Accessed 7/5/2015

[40] Smiley, Robert F., and Walter B. Horne. "MECHANICAL PROPERTIES OF PNEUMATIC TIRES WITH SPECIAL REFERENCE TO MODERN AIRCRAFT TIRES." (1958).

[41] Chen, Bo-Chiuan, and Huei Peng. "A real-time rollover threat index for sports utility vehicles." American Control Conference, 1999. Proceedings of the 1999. Vol. 2. IEEE, 1999.

[42] Eger, Ralf, and Uwe Kiencke. "Modeling of rollover sequences." Control Engineering Practice 11.2 (2003): 209-216.

[43] M. Pilgrim, “Intro to HFDM.” 2014.url: http://www.ihst.org/Portals/54/presentations/08_Intro_to_ HFDM_Mike_Pilgrim.pptx, accessed 7/15/2015

[44] Leishman, J. Gordon. Principles of Helicopter Aerodynamics with CD Extra. Cambridge university press, 2006.